JOURNAL OF MATERIALS SCIENCE 27 (1992) 4967–4973

Liquid-phase sintering in the glass–cordierite system: particle size effect

JAU-HO JEAN, T. K. GUPTA
Alcoa Electronic Packaging, Alcoa Technical Center, Alcoa Center, PA 15069, USA

The effect of particle sizes of glass and ceramic filler on the densification kinetics of glass-filled ceramics has been studied using borosilicate glass–cordierite as the model system. Within the particle size range investigated, the densification is found to be significantly enhanced by increasing the cordierite size, reducing the glass size and increasing the green density. These results are attributed to both the increased driving force of densification by reducing the glass particle size and the decreased glass redistribution distance by either increasing the green density of compacts or increasing the particle size ratio between the cordierite and glass powders. In addition, a large cordierite-to-glass size ratio gives a dense, uniform microstructure of sintered body as a result of forming a homogeneous close packing of the low-melting glass phase around the refractory cordierite particles.

1. Introduction

Liquid-phase sintering has been phenomenologically classified into three stages: rearrangement, solution and precipitation, and solid-state sintering [1]. For insoluble systems such as W–Cu [2, 3], W–Ag [3] and Al_2O_3–glass [4, 5] the densification during liquid-phase sintering is primarily achieved in the first stage. For systems with high-viscosity melt, such as glass ($> 1 \times 10^5$ N s m^{-2}) in glass–ceramics, a combination of melt formation, melt redistribution and particle rearrangement processes are generally observed in the first stage of liquid-phase sintering [6, 7].

Important factors affecting the densification behaviour of the initial stage of liquid-phase sintering have been identified and studied extensively, such as the contact angle of liquid on solid [2, 3], liquid content [8–10] and particle morphology [9, 10]. However, the effects of particle size and green density on the initial stage of liquid-phase sintering have not been studied in detail. Kingery [8] proposed that the linear shrinkage in the initial stage of liquid-phase sintering is inversely proportional to the filler particle size, because the capillary pressure is assumed to be the only driving force. It is interesting to note, however, that the experimental results do not always follow the theoretical prediction of Kingery. In the W–Cu system [11], for example, no difference in densification was observed for the W particle size ranging from 62 to 220 μm. However, for diamond in a liquid Cu–Ag–Ti alloy [12] the densification rate varied with the diamond particle size to the $-1/4$ power. In the Al_2O_3–glass system it was recently [13] reported that the densification and densification rate increased with increasing alumina particle size. These reported differences in experimental observations led us to examine the effect of particle size on the initial stage of liquid-phase sintering.

In a previous investigation [7] the effects of glass content, sintering temperature, time-dependent contact angle and glass viscosity on the densification of the borosilicate glass–cordierite system were studied. It was found that the densification of the borosilicate glass–cordierite system mainly takes place in the initial stage of liquid-phase sintering at 800–900 °C. Both the densification and the densification rate increase with increasing sintering temperature or glass content. Based on activation energy analysis, the rate-controlling step during densification has been found to be the viscous flow of glass with contributions arising from both the viscous sintering of glass and the glass redistribution kinetics. It was also observed from microstructural development, densification results and contact angle–time data that the densification kinetics can be adequately described by melt infiltration kinetics with a time-dependent contact angle. The infiltration distance, x, as a function of time, t, has been expressed as [7, 14–18]

$$x^2 = \frac{\gamma a \cos\theta_\infty}{2\eta}\left(t - \frac{1}{\beta} + \frac{e^{-\beta t}}{\beta}\right) \quad (1)$$

with

$$\beta = k\gamma/\eta \quad (2)$$

where a is the capillary pore size, γ is the surface tension of the glass, η is the viscosity of the glass, θ_∞ is the equilibrium contact angle and k is a constant. β was determined from the results of contact angle as a function of time [7]. In Equation 1 it is obvious that a larger melt infiltration distance takes a longer infiltration time to reach the same densification, which in turn reduces the densification rate or even the amount of densification at a given time. Although the melt redistribution distance during sintering of a compact cannot be measured directly, it can be qualitatively

0022–2461

influenced by changing the processing parameters, such as the particle size, particle size ratio and green density. The present study was undertaken to evaluate the effects of these processing parameters on the melt infiltration distance and on the densification kinetics of the glass–cordierite system, and is a logical extension of our previous study [7].

2. Experimental procedure

The borosilicate glass used in this study had an approximate composition of 75 wt % SiO_2 and 25 wt % B_2O_3. The cordierite powder was obtained from ICD Co. (Lyndhurst, New Jersey, USA). Particle size distributions of borosilicate glass and cordierite were determined by sedimentation (Micrometrics, Norcross, Georgia, USA). X-ray diffraction (XRD) analysis was used to determine the crystallinity of the powders and sintered compacts. The specific surface areas of the powders were measured by the nitrogen Brunauer–Emmett–Teller (BET) method.

Various sizes of glass and cordierite powders were attained by controlling grinding and gravitational settling times. Scanning electron microscopy (SEM) showed that all powders were irregular, but not porous based on the specific surface area results.

Powders and 5 wt % polyethylene glycol binder (Union Carbide, Cleveland, Ohio, USA) were mixed in 1-propanol. The slurry was deagglomerated by a high-energy ultrasonic horn (Heat Systems, Farmingdale, New York, USA). Mixing was continued for 2 h using a Turbula mixer (Glen Mills, Maywood, New Jersey, USA). The powder mixture was dried, ground and uniaxially pressed at 9×10^6 N m^{-2} to make pellets 1.9 cm in diameter and 0.3 cm high. The green densities of the as-pressed samples were measured dimensionally and used to describe the densification behaviour.

Samples were sintered isothermally in air at 800–900 °C. They were pushed into the heating zone after binder burnout. A period of 2 min was allowed for the samples to equilibrate at the sintering temperature. After the completion of sintering the samples were air-quenched to room temperature. No cracks were observed visually.

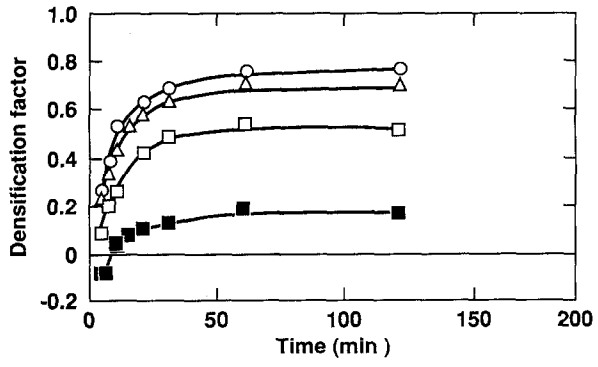

Figure 1 Densification factor versus time for 40 vol % glass with various C/G ratios at 825 °C: (○) 13.0/1.3 = 10.0, (△) 13.0/1.9 = 6.8, (□) 4.1/1.9 = 2.2 and (■) 4.1/14.5 = 0.28.

The sintered densities were determined by the Archimedes method. Samples were immersed in water, and the open pores were filled with water in vacuum for 2 h. The theoretical densities, 2.16 g cm^{-3} for the borosilicate glass and 2.55 g cm^{-3} for the cordierite, were used to calculate the theoretical densities of the pressed compacts by using the mixing rule. The pore size distribution of green compacts was measured by mercury porosimetry. Note that the pore size measurements on green compacts were conducted after the samples were fired at 500 °C for 60 min to remove binder completely. Microstructural changes during sintering were examined by SEM.

3. Results

3.1. Effect of particle size on densification

The effect of particle size on densification in this paper has been expressed in terms of the size ratio of cordierite to glass (C/G) particles. The densification behaviour is described as densification factor versus time, and the densification factor, DF, is defined as [1]

$$DF = (D_t - D_g)/(D_{th} - D_g) \quad (3)$$

where D_t is the instantaneous sintered density, D_g is the green density of the as-pressed compact and D_{th} is the theoretical density of the sintered compact calculated by the mixing rule. Although the green density of the compact after binder burnout should be used in Equation 3, there is difficulty in obtaining reliable densities because of the fragility of compacts, and hence we used the density of the as-pressed compacts. Fig. 1 shows the densification factor versus time at various C/G ratios for the system with 40 vol % glass and 60 vol % cordierite at 825 °C. For clarity of the graph, the data are shown for selected size ratios. The data for other size ratios show the same trend. It is seen that the densification factor increases with C/G ratio increasing from 0.28 to 10. In addition, the densification behaviour follows a similar pattern for all size ratios: densification takes place rapidly initially, slows down and then stops at a constant densification factor. Similar phenomena are also observed at other sintering temperatures from 800 to 900 °C. Since the densification factor remains nearly constant after firing for longer than 60 min, the densification factor at 60 min was arbitrarily selected as a measure of the constant densification factor. Fig. 2a shows that the constant densification factor at 825 and 850 °C increases by a factor of 0.2–0.3 when the cordierite size increases from 4 to 7 μm with glass size remaining constant at 1.9 μm. However, no significant change was observed for cordierite size > 7 μm. At the lowest temperature of sintering of 800 °C there was only a mild increase in the densification factor with cordierite size. In contrast with the effect of the particle size of the ceramic filler (cordierite), the effect of the particle size of glass is distinctly different. Fig. 2b shows that the constant densification factor decreases with increasing glass size at all temperatures when the cordierite size is kept constant. The results shown in Fig. 2 are replotted in Fig. 3 as constant densification

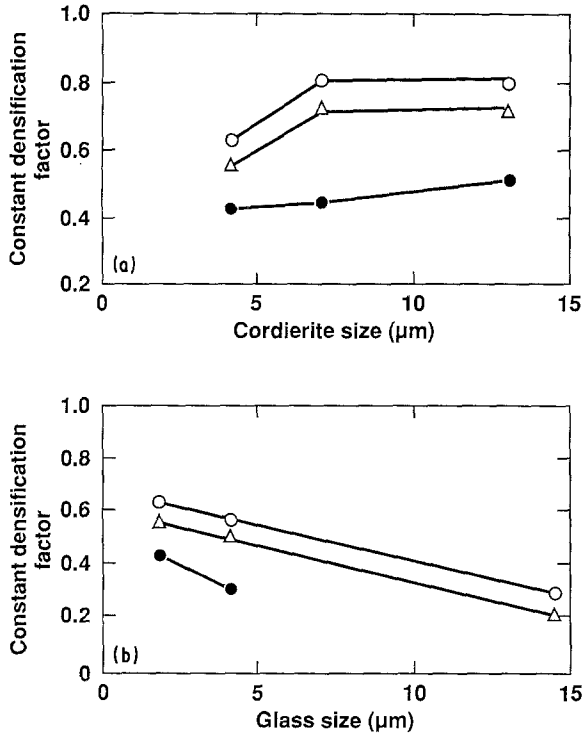

Figure 2 Constant densification factor versus (a) cordierite size (glass size 1.9 μm and sintering time 60 min) and (b) glass size (cordierite size 4.1 μm, sintering time 60 min) for 40 vol % glass at (○) 850, (△) 825 and (●) 800 °C.

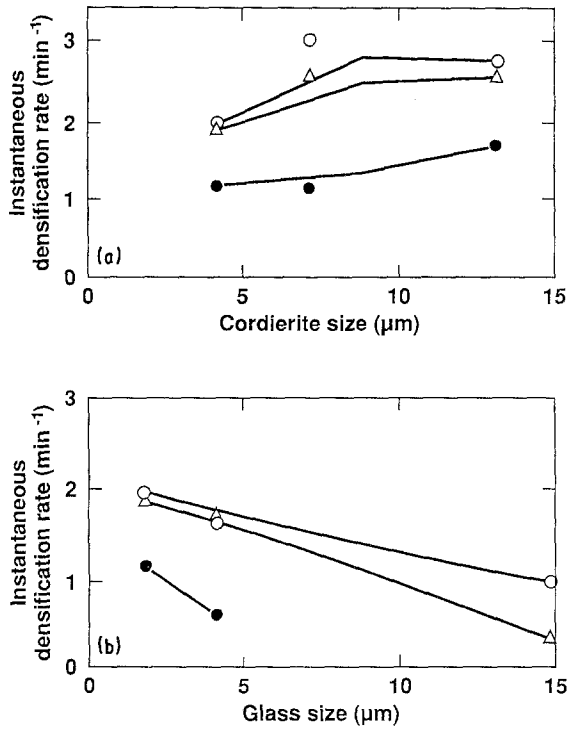

Figure 4 Instantaneous densification rate versus (a) cordierite size (glass size 1.9 μm) and (b) glass size (cordierite size 4.1 μm) for 40 vol % glass at (●) 800, (△) 825 and (○) 850 °C.

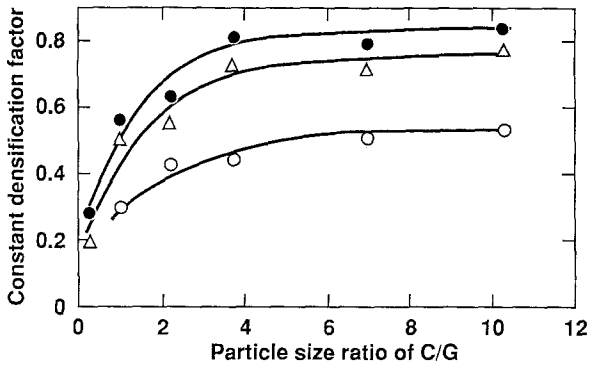

Figure 3 Constant densification factor as a function of particle size ratio of C/G for 40 vol % glass at (○) 800, (△) 825 and (●) 850° C, Sintering time 60 min.

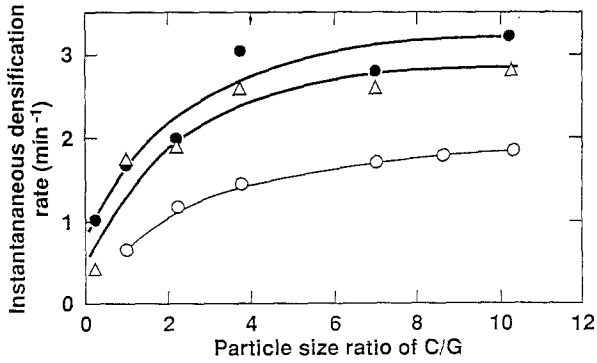

Figure 5 Instantaneous densification rate as a function of particle size ratio of C/G for 40 vol % glass at (○) 800, (△) 825 and (●) 850 °C.

factor versus C/G ratio at temperatures from 800 to 850 °C. It was found that the constant densification factor increases with increasing C/G ratio at the temperatures investigated.

The instantaneous densification rate on the rapidly rising part of Fig. 1 was determined by differentiating a curve-fitting equation to experimental densification–time plot. The results of the instantaneous densification rate at 10 min are presented in Figs 4 and 5. It was found that the dependence of the densification rate on the particle sizes of cordierite (Fig. 4a) and glass (Fig. 4b), and C/G ratio (Fig. 5) at various sintering temperatures are similar to those of the constant densification factor, i.e. increasing with increasing cordierite size, decreasing with increasing glass size and increasing with increasing C/G ratio within the size range studied.

3.2. Effect of green density on densification

The green densities of the compacts, prepared at the same pressure but different C/G ratio, are given in Fig. 6 (curve a) for the system with various glass contents. Note that the C/G ratio was extended to a value of 37 for these experiments. At a given C/G value no significant difference in green density for the systems with different glass content is observed. The results also show that the green density increases with increasing C/G ratio, from 57% at C/G = 1.0 to 67% at C/G = 10. No significant change in green density was found for C/G ratio ranging from 10 to 37. For comparison, sintered densities for various C/G values and glass contents at 850 °C for 60 min are also shown in Fig. 6 (Curves b to e). For all of the compositions investigated the results of sintered density versus C/G ratio generally have the same trend: initial increase

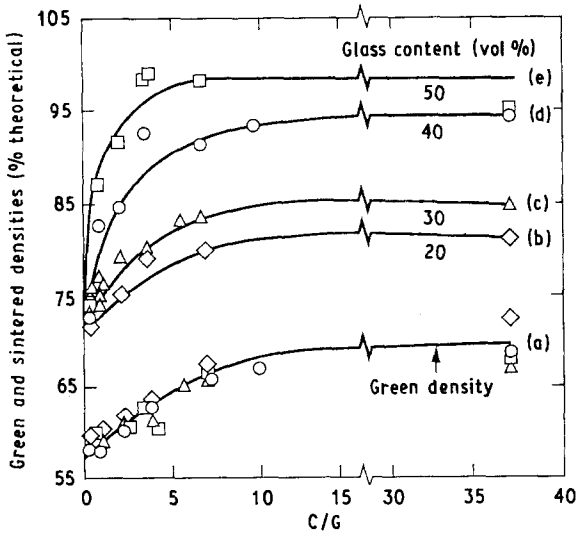

Figure 6 (a) Green density as a function of C/G ratio for various glass contents, and sintered density at 850 °C for 60 min at various glass contents: (b) 20, (c) 30, (d) 40 and (e) 50 vol %.

with C/G ratio, then reaching a constant sintered density. As the glass content increases at a given C/G ratio, the sintered density also increases. In addition, the sintered density reaches the constant value at a decreasing ratio of C/G as the glass content is increased.

4. Discussion

4.1. Effect of particle size on redistribution distance

It is important to mention at the beginning that the results presented in this paper are in agreement with our previous studies [7], i.e. the sintered density increases with increasing glass content and sintering temperature. In this discussion we highlight the importance of the cordierite and glass sizes, and the effect of the size ratio on the glass redistribution distance, densification and activation energy of densification.

The inverse relationships between glass size and densification (Fig. 2b), and instantaneous densification rate (Fig. 4b) are attributed to the fact that the driving force for the viscous sintering of glass is reduced as the glass size is increased. In addition, the glass redistribution distance is also increased with increasing glass size, which can also contribute to a reduced densification. Based on this interpretation, the linear relationship between the cordierite size and densification (Fig. 2a) and instantaneous densification rate (Fig. 4a) can be attributed to a smaller glass redistribution distance, resulting from a better packing of smaller glass particles around the cordierite particles. This explanation also applies to the rising part of the sintered density in Fig. 6. However, for the constant part of the densification curve the increase in C/G ratio seems to offer no further advantage, although the effect of increasing amount of glass is readily evident: the higher the amount of glass, the higher the rate of rise of density with respect to C/G ratio in the rising part as well as the magnitude of density in the constant part, as expected [7].

It is clear from the above discussion and from inspection of Fig. 6 that for a given glass content there is a critical value of the C/G ratio beyond which there is no significant reduction in the glass redistribution distance. Implicit in this conclusion is the fact that under this circumstance no further reduction in the redistribution distance is possible through particle packing density alone, i.e. the glass particles are now as densely packed around the cordierite particles as is practically possible. This is partly evinced in the plot of green density versus C/G ratio in Fig. 6; very little increase in green density occurs at C/G > 10. There are several ways to achieve a critical value of C/G ratio at which the redistribution distance seems to remain unchanged. Referring to Fig. 6, it is found that at a given glass volume, as the cordierite particle size is incrementally increased (to increase C/G), a critical value of C/G may soon be reached beyond which the mixture can be visualized as a matrix of fine glass particles surrounding the individually dispersed coarse cordierite particles, and the glass redistribution distance can be considered essentially constant for all practical purposes. In this case the redistribution distance can be assumed to be equivalent to the order of the pore size of the compact. It follows further from this argument that as the glass content of the mixture is increased (Fig. 6), this critical value will be attained at a lower C/G ratio. Experimentally the critical value of the C/G ratio can be determined from the intersection of two arbitrarily selected slopes, one from the constant densification part and the other from the rising part of the densification versus C/G curve, as shown in Fig. 6 curves b to e. It was found that the critical C/G values are 7–10 for 20 vol %, 5–7 for 30 vol %, 3–5 for 40 vol % and 2–4 for 50 vol % glass, and decrease with increasing glass content.

To assess the critical value of C/G at a given glass content quantitatively, we consider the relationship between the C/G ratio and the glass infiltration distance from the binary mixture packing viewpoint. Assuming that the powders are spherical and monosized, the ratio of particle numbers of glass to cordierite can be determined from the ratios of volume fraction and particle size

$$N_g/N_c = (V_g/V_c)(C/G)^3 \quad (4)$$

where N_g is the particle number of glass, N_c is the particle number of cordierite, V_g is the volume fraction of glass and V_c is the volume fraction of cordierite, which is equal to $1 - V_g$. The critical value of C/G can be obtained by equating this number ratio of N_g/N_c to the co-ordination number of cordierite (N_{coord}). The co-ordination number of the cordierite depends on the amount and size ratio of the particles. As the C/G ratio increases, the packing co-ordination of the cordierite particle also increases and the relationship is [19]

$$N_{coord} = 3.0 + 3.16(C/G)^2 \quad (5)$$

Equation 5 was derived from computer simulation, assuming spherical and monosized particles, and an optimum packing [19]. A relationship between glass content and the critical C/G value can be determined

by equating Equations 4 and 5, and expressed as

$$[V_g/(1 - V_g)] = [3 + 3.16(C/G)_{ct}^2](C/G)_{ct}^{-3} \quad (6)$$

where $(C/G)_{ct}$ is the critical value of C/G at a given glass content. The result of Equation 6 is shown as $(C/G)_{ct}$ versus V_g in Fig. 7, combined with the experimental results obtained earlier from Fig. 6. As noted, both calculated and experimental results show that $(C/G)_{ct}$ decreases as the amount of glass increases, although there is a discrepancy in magnitude between these two results. Furthermore, above the full curve the densification is complete, below incomplete.

For the cases with $C/G < (C/G)_{ct}$ (below the full curve in Fig. 7), in which the number of glass particles is not enough to completely surround the cordierite particles, the glass infiltration distance is equal to the product of geometrical glass particle separation and tortuosity [20]. This distance can be assumed to be no less than the cordierite particle size (4.1 μm in this study). This is shown schematically in inset a of Fig. 7 for an extreme case of C/G = 0.25 where the infiltration distance extends to several cordierite particle sizes. For the cases of $C/G > (C/G)_{ct}$ (above the full curve in Fig. 7) the glass redistribution distance is equal to the separation distance between glass particles and can be approximated by the pore size of the green compact, as shown schematically in inset b of Fig. 7 for a typical example of C/G = 4. Experimental results of the pore size distribution in this region measured by mercury porosimetry show that the pore size distribution and the median pore size of 40 vol % borosilicate glass do not show a significant change with C/G ratio, from 0.2 to 2 μm (x in Equation 1) and 0.52 μm ($2a$ in Equation 1) for C/G = 2.2 to 0.15–1.5 μm (x in Equation 1) and 0.43 μm ($2a$ in Equation 1) for C/G = 10. This variation in pore size distribution does not change the melt infiltration time significantly, e.g. from 55–540 s for C/G = 2.2 to 45–490 s for C/G = 10 at 850 °C, according to Equation 1 and the data shown in Table I [7]. Therefore, it can be expected, as is observed in the constant-densification part of the curves in Fig. 6, that the densification and densification rate remain relatively unchanged with respect to the C/G ratio for $C/G > (C/G)_{ct}$.

Inspection of Fig. 7 indicates that for a given volume of glass, as the cordierite particle size is increased with a corresponding increase in C/G ratio, a transition from $C/G < (C/G)_{ct}$ to $C/G > (C/G)_{ct}$ is also possible. This means that for a given volume of glass the infiltration distance can be reduced and the density increased simply by increasing the cordierite particle size or decreasing the glass particle size, i.e. by increasing the C/G ratio. This interpretation explains why the observed densification (Fig. 6) always increases in the rising part of the curve as the C/G ratio increases for $C/G < (C/G)_{ct}$.

4.2. Effect of particle size on the densification mechanism

The apparent activation energy of densification can be determined from an Arrhenius analysis, in which the plots are constructed using the logarithm of the specific rate T/t (K min^{-1}) at a constant densification factor versus $1/T$ (K^{-1}). The activation energies are then determined from the slopes by a least-squares fit method. Taking the system with C/G = 4.1/1.9 = 2.2 as an example, the apparent activation energies are (kJ mol^{-1}) 347 for DF = 0.4, 341 for DF = 0.35, 336 for DF = 0.3 and 332 for DF = 0.25, as obtained from the plot in Fig. 8. Table II lists the calculated apparent activation energies for the systems with different values of C/G. It is found that the apparent activation energies remain unchanged for C/G ratio increasing from 2.2 to 6.8, and are close to that of the viscous flow of borosilicate glass (290–310 kJ mol^{-1}) found in our

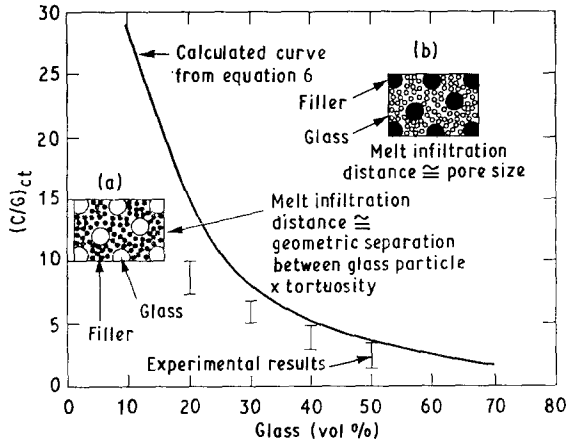

Figure 7 Critical value of C/G ratio as a function of glass content, and inset (a) schematic drawing of C/G = 0.25 and (b) C/G = 4. Note that above the full curve gives complete densification, below incomplete.

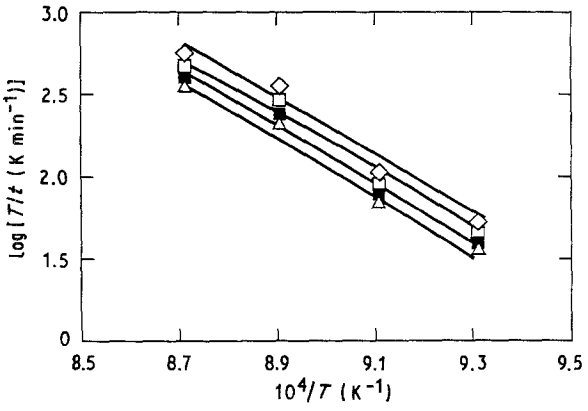

Figure 8 Plot of $\log(T/t)$ versus $1/T$ for 40 vol % glass and 60 vol % cordierite at various densification factors for C/G = 2.2: (◇) 0.25, (□) 0.30, (■) 0.35 and (△) 0.40.

TABLE I Values of the variables used to calculate infiltration distance in Equation 1 [7]

	Temperature (°C)				
	800	825	850	875	900
η ($\times 10^5$ N s m^{-2})	29.0	14.0	6.6	3.3	1.76
θ_∞ (deg)	34.5	33.2	32.0	34.1	27.2
β ($\times 10^{-3}$ s^{-1})	0.14	0.29	0.62	1.23	2.32

TABLE II Apparent activation energies (kJ mol^{-1}) of densification for different values of C/G

DF	C/G ratio		
	6.8	2.2	0.28
0.05			548
0.10			498
0.20	326		
0.25	351	334	
0.30	326	334	
0.35	334	343	
0.40		347	

earlier studies of the same system [7]. This result indicates that the rate-controlling step is the viscous flow of glass, and does not change with C/G ratio ranging from 2.2 to 6.8. However, a larger apparent activation energy is attained with a smaller C/G ratio, e.g. from 335 kJ mol^{-1} for C/G = 4.1/1.9 = 2.2 to 540 kJ mol^{-1} for C/G = 4.1/14.5 = 0.28. This result can be attributed to the large glass size and poor packing density of glass around cordierite, which either results in a smaller driving force or creates a greater viscous drag for particle rearrangement during densification. More importantly, the glass redistribution distance increases with increasing glass size at a given glass content, which can also contribute to slowing down the densification kinetics and thus increasing the apparent activation energy of densification. A similar result was also reported in the W–Cu system [21], in which a smaller activation energy of 120–210 kJ mol^{-1} was obtained for fine coreduced powders than that of 170–380 kJ mol^{-1} for coarse comixed powders.

4.3. Effect of particle size on the microstructure

To illustrate the effect of the particle size ratio between cordierite and glass on the sintered microstructure, samples with the same composition (40 vol % glass and 60 vol % cordierite) were fired at 900 °C for 60 min, at which the densification essentially stops and an equilibrium microstructure is obtained. With a given glass size (1.9 μm) SEM micrographs for the systems with 13.0, 7.0 and 4.1 μm cordierite are shown in Fig. 9a to c, respectively. Note that the round pores are uniformly distributed, indicating that the initial packing of glass was homogeneous, and extensive densification took place during firing. It was also found that the porosity and pore size, estimated from SEM micrographs, increased with decreasing cordierite size. Fig. 9d to f shows the microstructure of the systems with a constant cordierite size (4.1 μm) but with increasing glass size, 4.1, 8.6 and 14.5 μm, respectively. Obviously, the densification was substantially reduced by increasing the glass size. A slight increase in pore size with an increase in glass size was also observed. For 14.5 μm glass, however, a very inhomogeneous and porous sintered microstructure with large glass pools, distinct cordierite grains and sharp-edged pores was observed. Clearly, with a larger glass

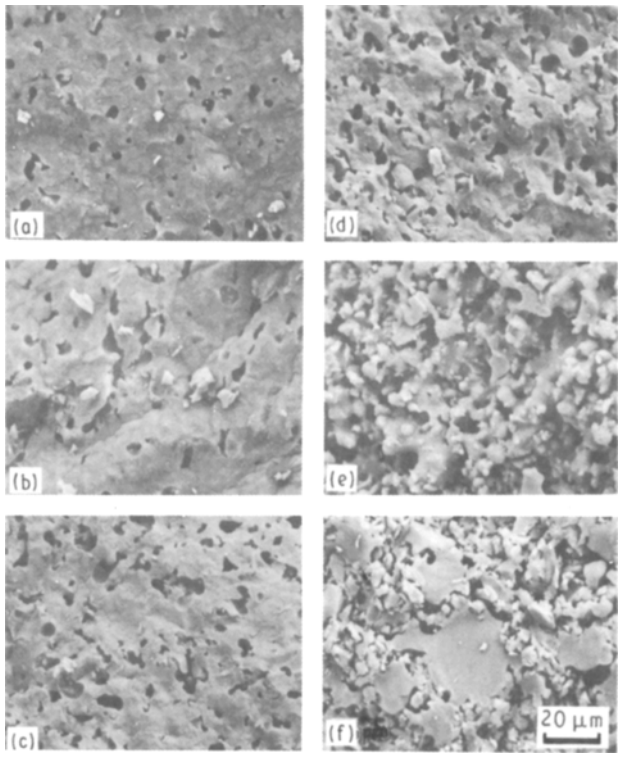

Figure 9 Microstructures for the systems with different C/G ratios at 900 °C for 60 min: (a) C/G = 13/1.9 = 6.8, (b) 7/1.9 = 3.7; (c) 4.1/1.9 = 2.2, (d) 4.1/4.1 = 1.0, (e) 4.1/8.6 = 0.48 and (f) 4.1/14.5 = 0.28.

size, a poorer densification, associated with limited glass redistribution and poor particle packing, takes place during sintering. The microstructural observations are thus consistent with the arguments presented in relation to Fig. 7.

5. Conclusions

The effect of the particle sizes of glass and ceramic filler on densification, densification rate, densification mechanism and microstructural development of glass-filled ceramics was studied using a borosilicate glass–cordierite system. Within the particle size range investigated a faster and greater densification, and a more uniformly densified microstructure, were observed with increasing cordierite size, decreasing glass size, increasing C/G ratio and increasing green density. These results are explained by an increased driving force of densification with a reduced glass particle size, and a reduced redistribution distance of the low-melting glass phase around the refractory cordierite phase as either the C/G ratio or the green density is increased. The apparent activation energies of densification for systems with C/G ratio in the range 2.2–6.8 were found to be very close to that of viscous flow of borosilicate glass, suggesting that the densification is controlled by the viscous flow of glass. However, a large activation energy was observed for the small C/G ratio of 0.28, which was explained by considering a larger glass redistribution distance, a greater viscous drag for particle rearrangement or a smaller driving force for densification. Finally, it was qualitatively shown that in order to obtain a high

density of the composite it is important to maintain a high degree of packing homogeneity and packing density of the borosilicate glass particle around the cordierite particle. In this study this condition is described by invoking a critical value of C/G ratio for a given volume of glass content in the composite.

Acknowledgement

The authors are pleased to acknowledge the contributions of C. Sell, J. Barker and K. Tipinski.

References

1. H. S. CANNON and F. V. LENEL, in Proceedings of the Plansee Seminar, edited by F. Benesovsky (Metallwerk Plansee, Reutte, 1953) p. 106.
2. W. J. HUPPMANN and H. RIEGGER, *Acta Metall.* **23** (1975) 965.
3. V. N. EREMENKO, Y. V. NAIDICH and I. A. LAVRINENKO, in "Liquid phase sintering" (Consultants Bureau, New York, 1970) ch. 4.
4. W. D. KINGERY, E. NIKI and M. D. NARASIMHAN, *J. Amer. Ceram. Soc.* **44** (1961) 29.
5. K. G. EWSUK, L. W. HARRISON and F. J. WALCZAK, in "Ceramic transactions", Vol. 1, edited by G. L. Messing, E. R. Fuller and H. Hausner, Jr (American Ceramic Society, Westerville, Ohio, 1988) p. 969.
6. R. M. GERMAN, in "Liquid phase sintering" (Plenum Press, New York, 1985) ch. 4.
7. J. H. JEAN and T. K. GUPTA, *J. Mater. Sci.* in press, 1992.
8. W. D. KINGERY, *J. Appl. Phys.* **30** (1959) 301.
9. K. S. HWANG, PhD thesis, Rensselaer Polytechnic Institute, Troy, New York (1984).
10. J. W. CAHN and R. B. HEADY, *J. Amer. Ceram. Soc.* **53** (1970) 406.
11. W. J. HUPPMANN, H. RIEGGER, W. A. KAYSSER, V. SMOLEJ and S. PEJOVNIK, *Z. Metallkde* **70** (1979) 707.
12. Y. V. NAIDICH, I. A. LAVRINENKO and V. A. EVDOKIMOV, *Soviet Powder Metall. Metal Ceram.* **11** (1972) 715.
13. K. G. EWSUK and L. HARRISON, in Proceedings of the Third International Conference on Ceramic Powders Processing Science, 1990, in press.
14. D. H. R. SARMA, PhD thesis, Purdue University, West Lafayette, Indiana (1982).
15. R. A. GREENKORN and D. P. KESSLER, in "Transfer operations" (McGraw-Hill, New York, 1972) p. 59.
16. I. H. SHAMES, in "Mechanics of fluid" (McGraw-Hill, New York, 1962) p. 94.
17. J. R. LIGENZA and R. B. BERSTEIN, *J. Amer. Chem. Soc.* **73** (1951) 4636.
18. J. SZEKELEY, A. W. NEUMANN and Y. K. CHUANG, *J. Collid Interf. Sci.* **35** (1971) 273.
19. R. BEN AIM and P. LE GOFF, *Powder Technol.* **2** (1968) 1.
20. P. LE GOFF, D. LECLERE and J. DODDS, *ibid.* **42** (1985) 47.
21. K. V. SEBASTIAN and G. S. TENDOLKAR, *Powder Metall. Int.* **11** (2) (1979) 62.

Received 16 May
and accepted 10 September 1991